

## Application Note # EBSD-01

# Fast simultaneous EBSD and EDS measurements for complete analysis of multiphase materials

The multi phase material used for this application note, i.e. high speed steel (HSS) is part of a family of alloys used mostly for producing cutting tools. Their name represents the synthesis of two of their most important characteristics:

- These alloys are part of a multi-component system Fe-C-X where X represents a group of alloying elements among which the most important are: Cr, W, Mo, V and for certain grades Co.
- The most important property of these alloys is their capability of retaining a very high hardness, even in the high temperature ranges resulting from the high speed metal cutting process.

Since their introduction most of the research was concentrated on understanding the formation and stability of carbides during manufacturing, in order to control the final mechanical properties of these steels, e.g. hardness, wear, etc.

GULYAEV et al. have proposed a discussion on the stability of the different types of carbides forming in HSS, based on the atomic layer filling of each element [1]. In their work GULYAEV et al. consider that the stability of carbides

in steels decreases with the increasing element group number. In other words, only the transition metals positioned on the left hand side of Fe in the table of elements can form carbides in steels, i.e. replace the fairly unstable cementite ( $\text{Fe}_3\text{C}$ ).

For the last few decades different techniques, such as X-ray diffraction, optical and electron microscopy etc. have been used for identifying/analyzing the different types of carbides present in HSS. Although the information given by these techniques is well established recent developments in speed and integration of the EBSD and EDS techniques have created a tool that can deliver richer and easier to interpret experimental data.

The aim of this application note is to demonstrate that the latest developments in simultaneous EBSD/EDS data acquisition and interpretation have created a powerful analytical tool for characterizing multiphase materials.

## Sample preparation and SEM/EBSD/EDS parameters

A commercially available high speed steel HSS-652 rod (see concentration of most important elements in table 1 below) with ferritic matrix was cut in longitudinal section and ground down to SiC grit paper 1200.

Table 1: Concentrations of most important alloying elements in HSS-652 (at%)

W	Mo	V	Cr	C	Fe
6	5	2	4	0.9	~81

Subsequently the sample was mechanically polished with 3 and respectively 1  $\mu\text{m}$  diamond suspension, followed by a final 7 minutes polishing with colloidal silica. For the last stages of the polishing procedure special care had to be taken in order to reduce the formation of surface relief, i.e. reduced pressure and increased polishing time. The relief formation probability is particularly high on this type of materials due to the very big difference in hardness between the carbides and the ferritic matrix. In general topography has a negative influence on the hit rate and therefore is to be avoided.

### Setup

SEM type	ZEISS Supra 55 VP
EBSD detector	<i>eFlash</i> <sup>TM</sup>
EDS detector	XFlash <sup>®</sup> 5030

### Acquisition parameters

Acceleration voltage	20 kV
Beam current	~15 nA (120 $\mu\text{m}$ aperture, high current mode)
<b>Acquisition speed (EBSD &amp; EDS)</b>	<b>210 points/s</b>
Input/Output avg. count rate	620 kcps / 300 kcps
Average counts per point	~1500
Map size	800x600 pixels (48 x 36 $\mu\text{m}^2$ )
Pixel size (step size)	57 nm
<b>Acquisition time</b>	<b>~38 min</b>

The data storage methodology used by the CrystAlign<sup>TM</sup> software allows the user to launch the measurement without the need to identify all the phases present in the sample<sup>1</sup>. This unique feature of the CrystAlign<sup>TM</sup> software can be used to minimize the SEM occupation time.

<sup>1</sup> Of course, if one or more phases are known or their presence is to be checked then these phases should be used for indexing during data acquisition.

For the present case Fe bcc ( $\alpha$ -phase) and Fe fcc ( $\gamma$ -phase) were used for indexing during data acquisition. While the presence of ferrite was certain, the formation of austenite as a result of the thermo-mechanical manufacturing processes had to be investigated.

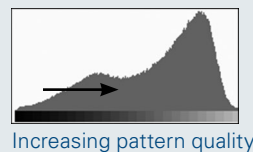
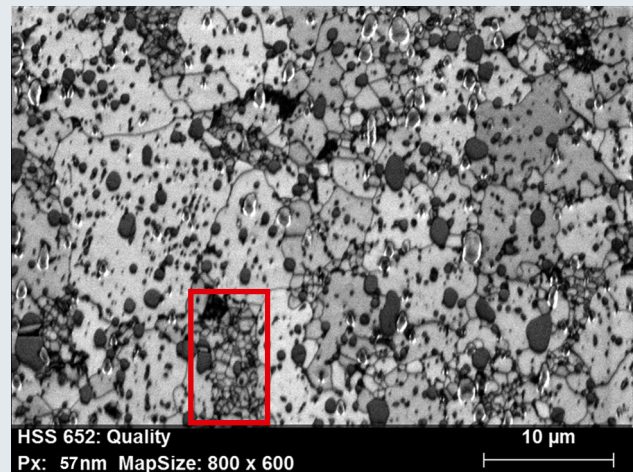
Due to the very finely scaled features observed by electron imaging a very fine step size had to be used, i.e. 57nm.

## Experimental results and discussion

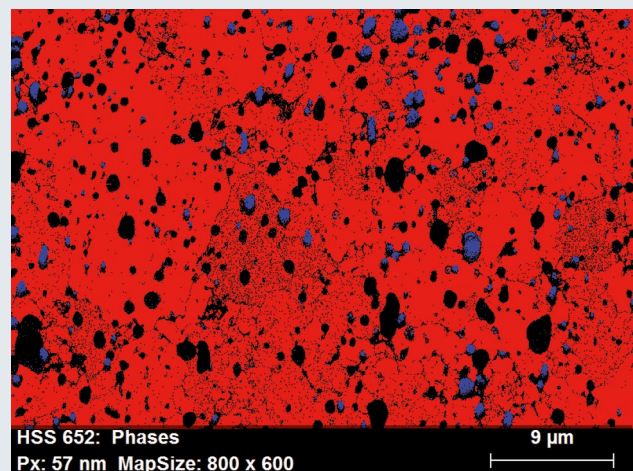
The microstructural features of the HSS sample used for this study are depicted by the pattern quality map (PQM) and phase distribution map shown in Figure 1.

The two maps indicate the presence of micron and

### Pattern quality and initial phase maps



a)



b)

Fig. 1: Pattern quality map (a) and “raw”– as acquired – phase map (b) showing the pixels indexed as ferrite (red) and austenite (blue); black pixels in the phases map denote points not indexed.

submicron scaled particles inside a ferritic matrix. The matrix appears to be characterized by recrystallized grains but local areas with fine structures/substructures are also visible in the PQM (see area indicated by the red rectangle in Figure 1 a)).

The raw phase map shown in Figure 1 b) represents the as acquired EBSD data, i.e. no data cleaning was applied. The map depicts the distribution of particles/grains that have been indexed as austenite (blue pixels) inside the ferritic matrix (red pixels). The black non-indexed areas in Figure 1 b) correspond to the particles having a lower pattern quality (i.e. darker grey level) compared to the matrix (see Figure 1.a)). These details indicate the existence of at least

another phase, which is either lighter than the ferrite or it has a lower crystallographic symmetry.

The information provided by the EDS results, through the Hypermap option, was used for identifying the missing phase(s) as well as for confirming the EBSD results. The Hypermap feature can be used, among other options, for displaying the element distribution within the scanned area. The W and Mo hypermaps shown in Figure 2 a) and b) respectively indicate that the non-indexed areas in Figure 1 b) are W and Mo rich.

A quick look into the literature and a search in a phase

### EDS maps and quantitative analysis results

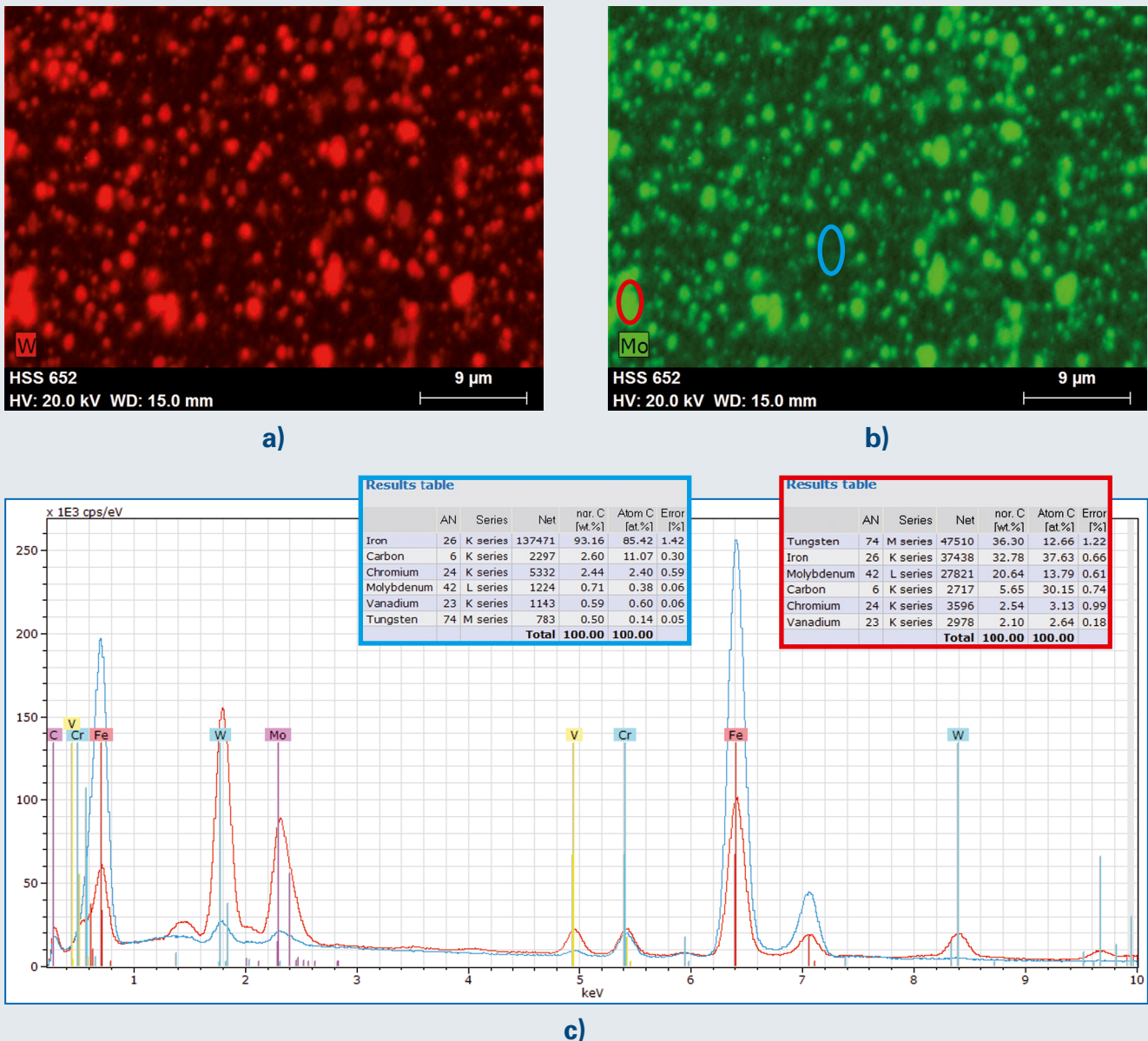
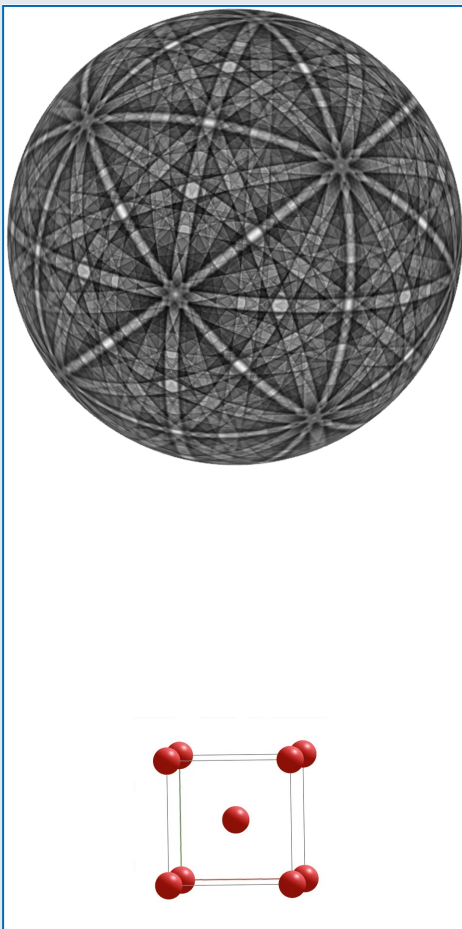


Fig. 2: Element distribution maps for W (a) and Mo (b). The EDS spectra as well as the quantitative results corresponding to the two areas indicated in (b) by red and light blue ovals, W, Mo-rich particle and matrix, are also shown.

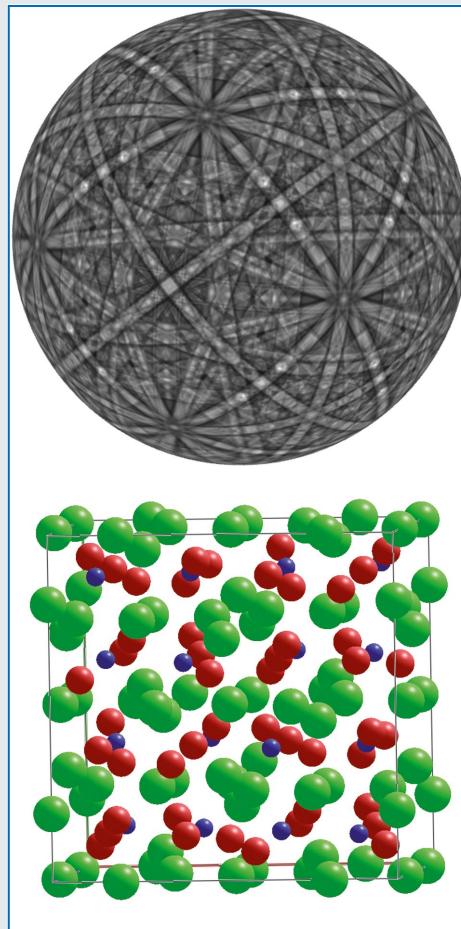


### Dynamically simulated patterns and unit cells



IT-No.: 229,  $a_0 = 2.866 \text{ \AA}$   
 $\rho = 7.88 \text{ g/cm}^3$

**a)**



IT-No.: 227,  $a_0 = 11.087 \text{ \AA}$   
 $\rho = 14.25 \text{ g/cm}^3$

**b)**

Fig. 3: Intensity distribution (dynamic theory simulation) on a projection sphere based on the given crystal structures for the matrix  $\alpha$ -Fe (a) and for the identified carbide  $W_3Fe_3C$  (b). Please note that the unit cell structures were scaled to depict the difference in lattice parameters.

database – e.g. the commercially available ICSD (Inorganic Crystal Structure Database) – confirms that the patterns acquired from the W and Mo rich particles are correctly indexed as an  $M_6C$  type<sup>2</sup> of carbide i.e.  $W_3Fe_3C$ . Considering the EDS quantification results (see Figure 2 c)), it is only logical to conclude that the real phase corresponding to these particles had part of the W and Fe atoms replaced by Mo atoms without changing the crystallographic structure as compared to the  $W_3Fe_3C$  phase.

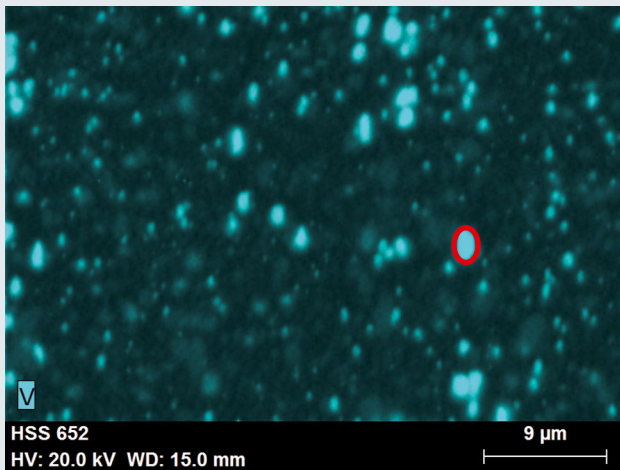
Figure 3 shows the different crystal structures of ferrite and  $W_3Fe_3C$ , as well as the corresponding predicted intensity distributions based on the kinematic approach. The structure and the intensity are related to the space-group symmetry (given by the IT-No.).

As stated above, the EDS results can not only be used for identifying the missing phases but also for confirming/correcting the phase information in the EBSD data. The element distribution maps of V and C shown in Figure 4 a) and b) respectively clearly indicate that the areas indexed as austenite (see Figure 1 b)) are V and C rich. As these high amounts of V and especially C (cf. quantification in Figure 4 c)) cannot be solved in austenite, one can only conclude that the areas actually correspond to a phase forming austenite-like EBSPs.

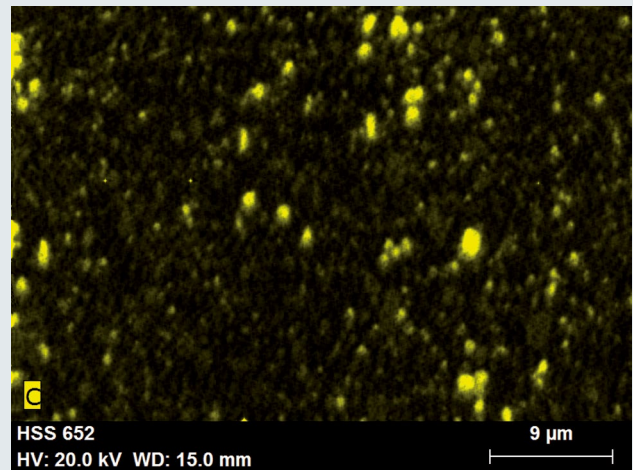
A similar search procedure as the one used for the  $M_6C$  phase, has found that there is indeed an MC type of carbide i.e. vanadium carbide VC which can be used to correctly index the patterns initially indexed as austenite. The MC type carbide is described by the NaCl crystal structure type.

<sup>2</sup> M is an abbreviation for „metal“.

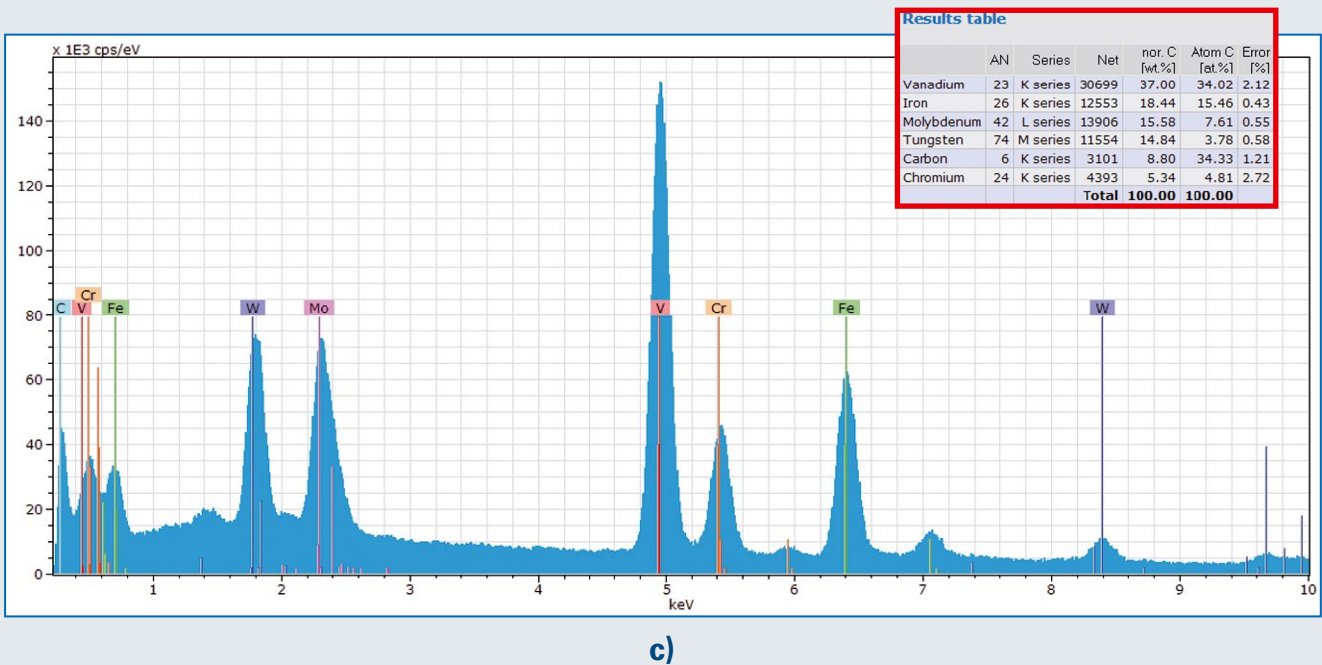
## EDS maps and quantitative analysis results



a)



b)



c)

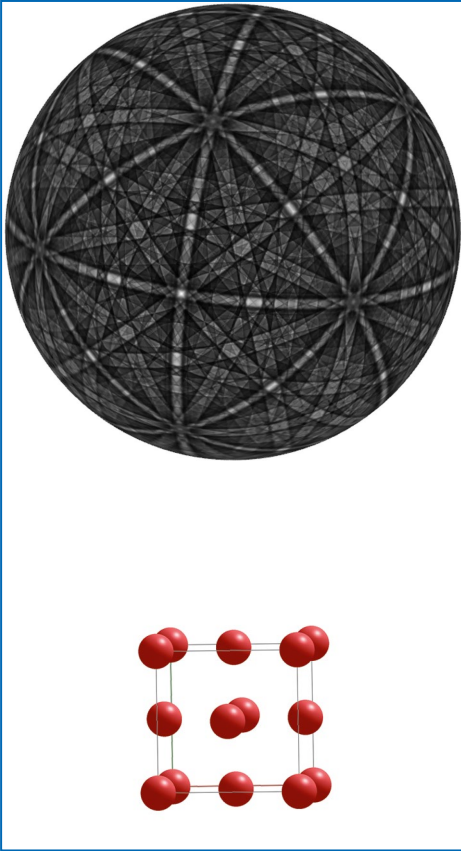
Fig. 4: Element distribution map for V (a) and C (b). The EDS spectrum and the quantitative results corresponding to the area indicated in a) by the red oval are shown in c).

The reason why the EBSD system cannot distinguish satisfactorily between austenite and vanadium carbide, is due to the same intensity ranking of the major bands corresponding to these two phases. This is the main criterion used during the indexing procedure by any existing EBSD system. Since their unit cell parameters differ only by about 13% a differentiation using the band widths could be practically possible, but only if extremely slow data acquisition of high resolution and high quality patterns were used. Fast automatic measurements usually do not offer this option, and since Hypermap simultaneously delivers a direct assessment of the chemical composition, it is therefore much more efficient to use the EDS results for identifying the correct phase.

After identifying the candidate phases, an offline reanalysis of the initial data was carried out. A speed of  $\sim 3000$  points/s was achieved during reanalysis using a dual quad core computer (eight processor cores). In other words: a map of 480,000 points was reanalyzed in about 2min30sec. A hit rate of 93.8% was achieved, indicating that a solution has been attributed to most of the points in the map. The two raw maps shown in Figure 6 confirm the reliability of the final results, i.e. extremely low to no phase or orientation misindexing present. Non-indexed pixels correspond mainly to areas showing weak or no EBSPs, see dark areas in the PQM in Figure 1 a).

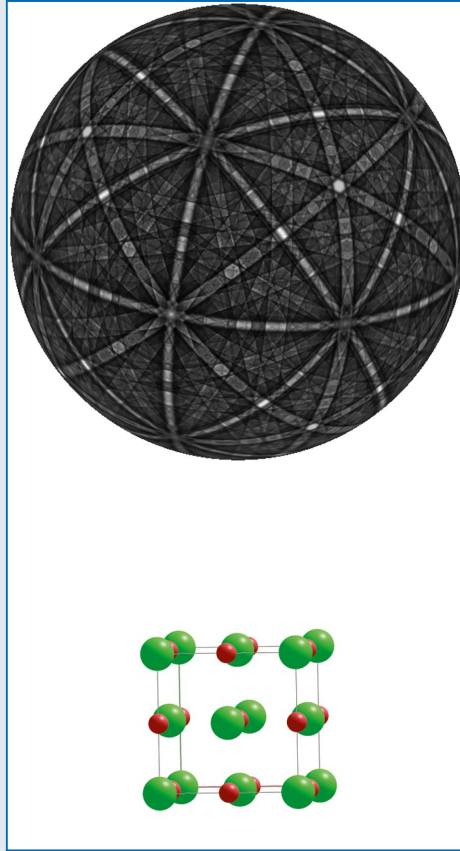


Dynamically simulated patterns and unit cells



IT-No.: 225,  $a_o = 3.66 \text{ \AA}$   
 $\rho = 7.57 \text{ g/cm}^3$

**a)**

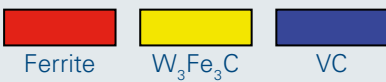
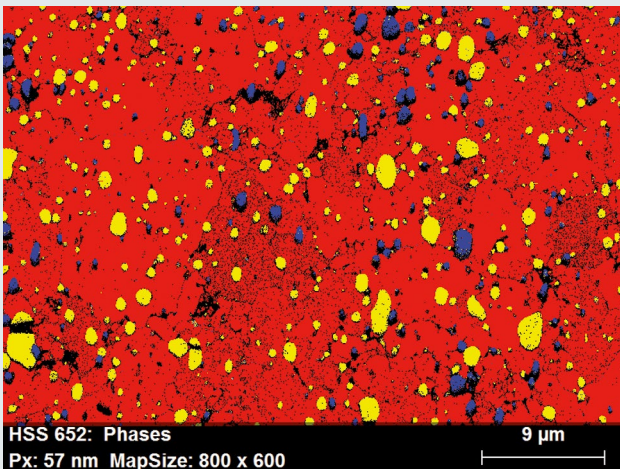


IT-No.: 225,  $a_o = 4.165 \text{ \AA}$   
 $\rho = 5.79 \text{ g/cm}^3$

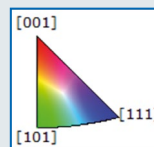
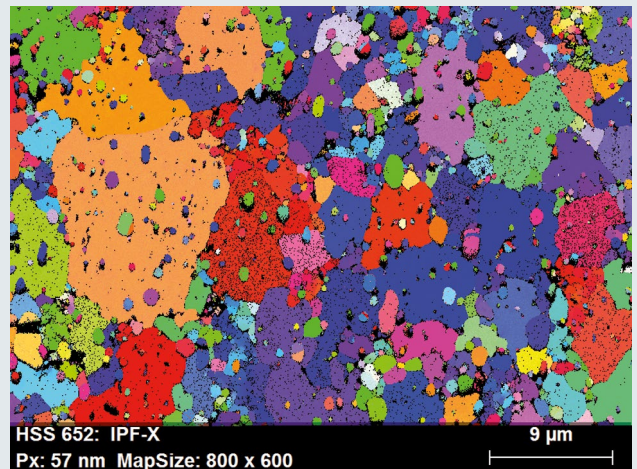
**b)**

Fig. 5: Comparison of the intensity distribution (dynamic theory simulation) on a projection sphere for austenite and vanadium carbide. Because of the similar crystal structures the intensity distributions are similar as well.

Phase and orientation maps



**a)**



**b)**

Fig. 6: Raw EBSD data after reanalysis: Phase map (a) and orientation map (b). Please note that no data cleaning was applied.

### EDS map, pattern quality and phase maps

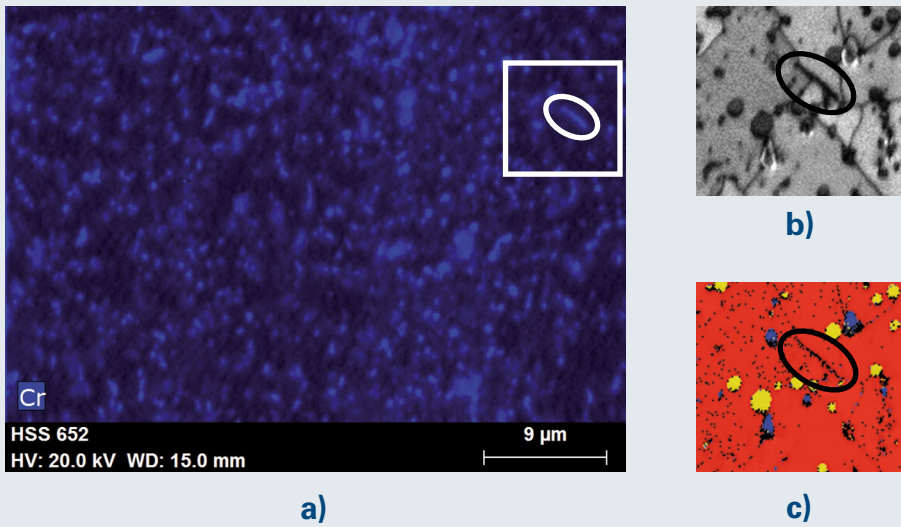


Fig. 7: Element map for Cr (a) and pattern quality map (b) with phase map (c) from the upper left hand side area, indicating the presence of Cr-rich precipitates at the grain boundaries of the ferritic matrix.

These regions are mostly situated at the boundary between the matrix and the carbides where the pattern quality is substantially decreased due to surface relief. Moreover, a few areas inside the matrix are characterized by extremely fine grains, so that one risks overstepping the spatial resolution limit given by the used experimental conditions (beam size, acceleration voltage, etc.).

A closer look at the Cr element map indicates the presence of Cr-rich particles at the grain boundaries of the ferritic matrix, cf. Figure 7. Unfortunately these areas do not show any EBSPs. The particle size appears to be extremely small, possibly below the spatial resolution of the EBSD technique.

Even though these precipitates could not be fully analyzed due to the limitations of the EBSD technique, it is important to note that the measurement has revealed their presence. Alternative techniques with better spatial resolution, e.g. TEM, could possibly be used to identify the nature of these precipitates.

The area fractions for each phase, as found by the present measurement, are depicted by the graph in Figure 8 a). These values are consistent with the values presented in the literature [2,3].

### Phase and particle size distributions

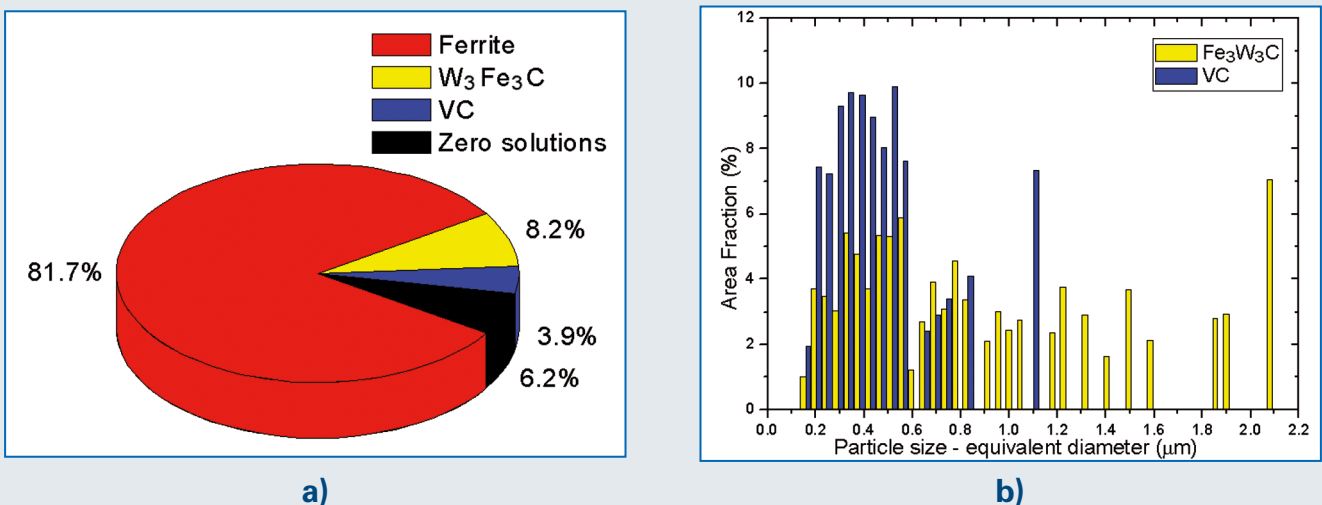


Fig. 8: Phase distribution statistics (a) and area weighted particle size distribution for the two types of carbides (b), i.e.  $M_6C$  and  $MC$ .

The area weighted particle size distribution is given in Figure 8 b). When measuring grain/particle sizes with EBSD [4] a grain/particle is defined by the minimum number of data points per grain, the threshold boundary misorientation angle and the step size. In the present case, a criterion of minimum 8 pixels per grain/particle<sup>3</sup> and a threshold misorientation angle of 5° has been used.

The results shown in Figure 8 b) indicate that the VC particles are submicron sized with an average particle size of ~400nm. The M<sub>6</sub>C-type carbides have particle sizes distributed over a wide range between 0.2 to 2.5 microns.

## Summary

Commercially available high speed steel was analyzed simultaneously using the EBSD and EDS techniques at a very high speed of more than 200 points/s. Thanks to its extremely fast reanalysis option the CrystAlign™ software permits the user to launch measurements without knowing all the phases present in the sample. This in turn significantly reduces the preparation time needed before launching the measurement. Thanks to these new hardware and software developments the SEM occupation time for acquiring a map of 480,000 points was drastically reduced to less than one hour i.e. 38 min for data acquisition, plus maximum 15 min for sample, electron beam, hardware and software setup.

As shown throughout this application note, the complete phase identification as well as the map reanalysis is done offline extremely fast and without occupying the SEM. Although the possibility of characterizing multi phase materials by using the EBSD and EDS techniques has been already available at least for the last ten years, this application note demonstrates that the combination of the Bruker EBSD and EDS detectors with the ESPRITsoftware results in a powerful and efficient analytical tool that can be used to easily and efficiently analyze multiphase materials, providing excellent results.

---

<sup>3</sup> F.J. Humphreys has shown that a minimum of 8 pixels per grain are required for an accuracy of 5% in determining the grain size [5].

## References

- [1] A.P. Gulyaev, Metal Science and Heat Treatment 40 (1998) 456.
- [2] S. Karagöz, H.F. Fischmeister, Metallurgical and Materials Transactions 29A (1998) 205, 1998.
- [3] T.A. Roik, Y.F. Shevchuk, Powder Metallurgy and Metal Ceramics 45 (2006) 531.
- [4] F.J. Humphreys, Scripta Materialia, 51 (2004) 771-776.
- [5] F.J. Humphreys, Journal of Material Science, 36 (2001) 3833.

## Author

Dr. Daniel Goran, Application Scientist EBSD,  
Bruker Nano GmbH

## Bruker Nano GmbH

Berlin · Germany  
Phone +49 (30) 670990-0  
Fax +49 (30) 670990-30  
info.bna@bruker.com

[www.bruker.com/quantax-ebds](http://www.bruker.com/quantax-ebds)

